

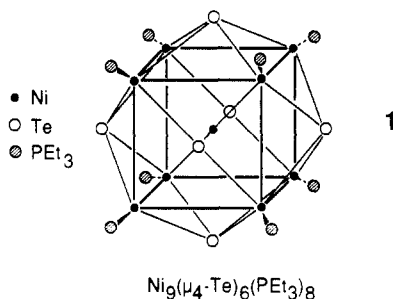
Bonding to Interstitial Main-Group or Transition-Metal Atoms in Cubic Clusters Related to $\text{Ni}_9(\mu_4\text{-Te})_6(\text{PEt}_3)_8$

Ralph A. Wheeler

Contribution from the Department of Chemistry and Biochemistry, 620 Parrington Oval, Room 208, University of Oklahoma, Norman, Oklahoma 73019. Received April 23, 1990

Abstract: The Te-centered, cubic cluster $\text{Ni}_8\text{Te}(\mu_4\text{-Te})_6(\text{L})_8$ is suggested as a stable molecule, on the basis of extended Hückel molecular orbital calculations for the cluster and its experimentally known, Ni-centered analogue, $\text{Ni}_9(\mu_4\text{-Te})_6(\text{PEt}_3)_8$. Calculations show that the interstitial Ni or Te atom binds to the empty cluster at the expense of Ni-Ni and Ni-Te bonding within the cluster framework. The interstitial Ni atom compensates by bonding weakly to the framework nickels, primarily through its a_{1g} (4s) orbital; the central Te bonds strongly to both the nickel cube and the face-capping telluriums. Large HOMO-LUMO gaps suggest that 130 or 114 electrons are optimum for $\text{Ni}_8\text{Te}(\mu_4\text{-Te})_6(\text{L})_8$. Analogies to the solid-state structures of NiTe and CsCl, as well as to the centered octahedral clusters $\text{Zr}_6\text{I}_{12}\text{Z}$ (Z = main-group or transition-metal atom), are pointed out.

Cluster chemistry is proving a meeting ground between the molecular and the solid-state chemist as each seeks to understand the transition from molecular to extended solids. An impressive array of clusters resembling pieces of an infinite solid have already been made by a variety of ingenious methods. These include 6-8 and 6-12 clusters¹ fused to form extended, solid-state structures and pieces of zinc and cadmium chalcogenide semiconductors synthesized inside zeolites, inverse micelles, and biological membranes.² Brennan, Steigerwald et al. produced yet another fascinating cluster compound when they intercepted the $\text{Ni}_9(\mu_4\text{-Te})_6(\text{PEt}_3)_8$ intermediate during their clever synthesis of solid NiTe from organometallic precursors.³ The $\text{Ni}_9(\mu_4\text{-Te})_6(\text{PEt}_3)_8$ cluster is shown in **1** and consists of a cubic arrangement of eight



nickel atoms with a ninth nickel at the cube's center. Each face of the nickel cube is capped by a tellurium atom. One terminal phosphine ligand completes the approximately tetrahedral coordination environment of each nickel located at the cube's corners.

A trigonal distortion is observed for the idealized, cubic $\text{Ni}_9(\mu_4\text{-Te})_6(\text{PEt}_3)_8$ cluster shown in **1** and prompted the authors of ref 3 to draw the analogy between $\text{Ni}_9(\mu_4\text{-Te})_6(\text{PEt}_3)_8$ and the extended NiTe structure. The distortion slightly contracts Ni-Ni distances along face diagonals of the cube to move toward a

trans-bicapped octahedral array of metals. The NiTe structure⁴ is obtained from the distorted cube by replacing the terminal phosphines in **1** by telluriums and noting the close-packed layers of nickel and tellurium along the cube's body diagonal.

So the $\text{Ni}_9(\mu_4\text{-Te})_6(\text{PEt}_3)_8$ cluster is interesting as a fragment of solid NiTe. In addition, $\text{Ni}_9(\mu_4\text{-Te})_6(\text{PEt}_3)_8$ is directly related to a number of clusters based on cubic transition-metal frameworks^{5,6} and, less directly, to octahedral clusters centered by transition-metal or main-group atoms.⁷ This latter analogy, to the centered octahedral clusters, hints at the possible stability of a cubic cluster encapsulating a main-group, rather than a transition-metal, atom. I investigate this provocative suggestion here and propose cluster electron counts appropriate to stabilize a tellurium-centered, cubic Ni cluster—a structure analogous to the solid-state structure of CsCl.⁸

Structural Analogies

The structural relationship between the $\text{Ni}_9(\mu_4\text{-Te})_6(\text{PEt}_3)_8$ cluster and the extended NiTe structure is clear; less clear is why the analogous cubic cluster related to CsCl and centered by tellurium, $\text{Ni}_8\text{Te}(\mu_4\text{-Te})_6(\text{L})_8$, has not yet been observed. This cluster and a piece of NiTe in the CsCl structure are displayed in **2**. These structures are similar to those shown in **1**, but differ primarily by having the Ni atom at the cube center replaced by Te. In the CsCl structure type illustrated in **2**, the terminal and face-capping telluriums actually occupy the centers of unit cells neighboring the central cubic cell.

The proposed $\text{Ni}_8\text{Te}(\mu_4\text{-Te})_6(\text{L})_8$ structure bears the same relationship to $\text{Ni}_9(\mu_4\text{-Te})_6(\text{PEt}_3)_8$ as main-group- and transition-

(1) The notation 6-8 refers to an octahedral cluster of six metal atoms with each of its eight faces capped. Likewise, 6-12 refers to an octahedron with a ligand bridging each of its 12 edges. Some leading references are as follows: (a) Schäfer, H.; Schnering, H. G. *Angew. Chem.* **1964**, *76*, 833. (b) Simon, A. *Angew. Chem.* **1981**, *93*, 23; *Angew. Chem., Int. Ed. Engl.* **1981**, *20*, 1. (c) Simon, A. *Angew. Chem.* **1988**, *100*, 163; *Angew. Chem., Int. Ed. Engl.* **1988**, *27*, 159. (d) Chevrel, R.; Sergent, M. In *Crystal Chemistry and Properties of Materials with Quasi-One-Dimensional Structures*; Rouxel, J., Ed.; D. Reidel: Dordrecht, 1986; p 315. (e) Corbett, J. D. *Pure Appl. Chem.* **1984**, *56*, 1527.

(2) (a) Steigerwald, M. L.; Brus, L. E. *Annu. Rev. Mater. Sci.* **1989**, *19*, 471. (b) Wang, Y.; Herron, N. J. *Phys. Chem.* **1987**, *91*, 257. (c) Meyer, M.; Wallberg, C.; Kurihara, K.; Fendler, J. H. *J. Chem. Soc., Chem. Commun.* **1984**, 90. (d) Dameron, C. T.; Reese, R. N.; Mehra, R. K.; Kortan, A. R.; Carroll, P. J.; Steigerwald, M. L.; Brus, L. E. *Nature* **1989**, *338*, 596.

(3) (a) Brennan, J. G.; Siegrist, T.; Stuczynski, S. M.; Steigerwald, M. L. *J. Am. Chem. Soc.* **1989**, *111*, 9240. (b) A related cluster, $[\text{Pd}_9\text{As}_6(\text{PPh}_3)_8]$, is described: Fenske, D.; Fleischer, H.; Persau, C. *Angew. Chem.* **1989**, *101*, 1740; *Angew. Chem., Int. Ed. Engl.* **1989**, *28*, 1665.

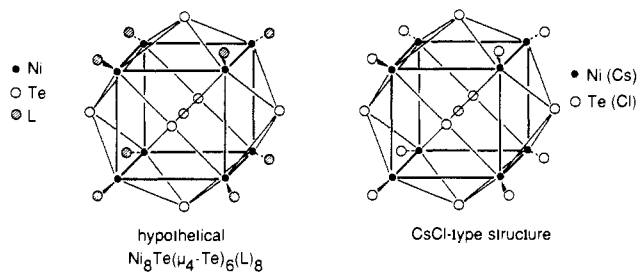
(4) (a) Dvoryankina, G. G.; Pinsker, Z. G. *Kristallografiya* **1963**, *8*, 556; *Sov. Phys. Crystallogr. Engl. Transl.* **1964**, *8*, 448. (b) See also: Pearson, W. G. *The Crystal Chemistry and Physics of Metals and Alloys*; Wiley-Interscience: New York, 1972; p 388.

(5) (a) Fenske, D.; Ohmer, J.; Hachgenei, J.; Merzweiler, K. *Angew. Chem.* **1988**, *100*, 1300; *Angew. Chem., Int. Ed. Engl.* **1988**, *27*, 1277. (b) Whitmire, K. *J. Coord. Chem.* **1988**, *17*, 95.

(6) (a) Lower, L. D.; Dahl, L. F. *J. Am. Chem. Soc.* **1976**, *98*, 5046. (b) Fenske, D.; Hachgenei, J.; Ohmer, J. *Angew. Chem.* **1985**, *97*, 684; *Angew. Chem., Int. Ed. Engl.* **1985**, *24*, 706. (c) Fenske, D.; Basoglu, R.; Hachgenei, J.; Rogel, F. *Angew. Chem.* **1984**, *96*, 160; *Angew. Chem., Int. Ed. Engl.* **1984**, *23*, 160. (d) Fenske, D.; Hachgenei, J.; Rogel, F. *Angew. Chem.* **1984**, *96*, 959; *Angew. Chem., Int. Ed. Engl.* **1984**, *23*, 982. (e) Christou, G.; Hagen, K. S.; Bashkin, J. K.; Holm, R. H. *Inorg. Chem.* **1985**, *24*, 1010. (f) Christou, G.; Hagen, K. S.; Holm, R. H. *J. Am. Chem. Soc.* **1982**, *104*, 1744. (g) Al-Ahmad, S. A.; Salifoglou, A.; Kanatzidis, M. G.; Dunham, W. R.; Coucouvanis, D. *Inorg. Chem.* **1990**, *29*, 927.

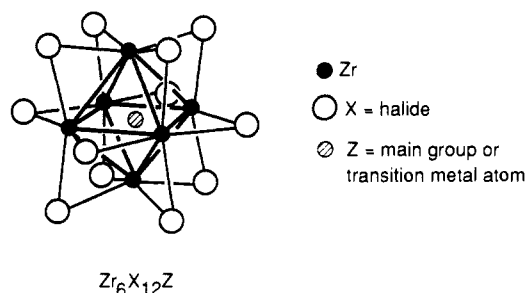
(7) (a) Ziebarth, R. P.; Corbett, J. D. *Acc. Chem. Res.* **1989**, *22*, 256 and references therein. (b) Smith, J. D.; Corbett, J. D. *J. Am. Chem. Soc.* **1985**, *107*, 5704. (c) Hughbanks, T.; Rosenthal, G.; Corbett, J. D. *J. Am. Chem. Soc.* **1988**, *110*, 1511. (d) Hughbanks, T.; Rosenthal, G.; Corbett, J. D. *J. Am. Chem. Soc.* **1986**, *108*, 8289. (e) Payne, M. W.; Corbett, J. D. *Inorg. Chem.* **1990**, *29*, 2246 and references therein.

(8) Reference 4a, pp 305ff.



2

metal-centered zirconium (or rare-earth) halides bear to each other. These compounds, displayed in 3, are well-known to cluster



3

chemists and have been extensively studied by Corbett and his co-workers.⁷ They are composed of octahedra of Zr (rare-earth) atoms bridged on each edge by a halide ligand. At the center of each octahedron rests a main-group or transition-metal atom. Bonding in these clusters is well understood, as are preferred electron counts and the reasons that the metal frameworks differ in the two structures.⁷

Unlike the analogous Zr or rare-earth halides, the proposed $\text{Ni}_8\text{Te}(\mu_4\text{-Te})_6(\text{L})_8$ cluster can accommodate the "interstitial" Te with minimal distortion of the cluster framework present in 1. This is so because Ni–Te and Te–Te distances for $\text{Ni}_8\text{Te}(\mu_4\text{-Te})_6(\text{L})_8$ are in the range of normal bond lengths. The central Te contacts the other telluriums at a distance of 2.98 Å, a distance longer than the Te–Te bond length in elemental Te (2.84 Å) but within the range of observed Te–Te contacts.⁹ Likewise, the Te–Ni distance of 2.47 Å is only slightly shorter than the 2.48-Å separation observed in NiTe films.^{4b} In this paper, I propose the structural stability of the CsCl analogue, $\text{Ni}_8\text{Te}(\mu_4\text{-Te})_6(\text{L})_8$ (shown in 2), and compare metal–metal and metal–ligand bonding in the two clusters, $\text{Ni}_9(\mu_4\text{-Te})_6(\text{PET}_3)_8$ and $\text{Ni}_8\text{Te}(\mu_4\text{-Te})_6(\text{L})_8$. But before we consider the bonding, let us look at the idea in light of what we already know about related cluster structures and their observed electron counts.

Since Lower and Dahl first synthesized $\text{Ni}_8(\mu_4\text{-PPh})_6(\text{CO})_8$,^{6a} a variety of cubic transition-metal clusters have been made and structurally characterized by a number of different groups.^{5,6} Table I lists some representative examples with their electron counts. The preferred electron count for closed-shell, cubic clusters is 120.¹⁰ This number is conveniently derived from the 40 electrons present in the organic cubane "cluster" plus 80 electrons carried by the d orbitals of eight transition-metal atoms. When present, a central atom is generally considered to donate all of its electrons to the cluster. 130 then becomes the preferred electron count for a cubic cluster centered by a transition-metal atom.

The electron count for $\text{Ni}_9(\mu_4\text{-Te})_6(\text{PET}_3)_8$ is included in Table I and is derived by first assigning a 2– formal charge to each Te.

(9) (a) Wells, A. F. *Structural Inorganic Chemistry*, 4th ed.; Clarendon: Oxford, 1975; Chapter 16, p 573. (b) The wide range of Te–Te bond distances found in a variety of compounds is discussed: Böttcher, P. *Angew. Chem.* **1988**, *100*, 781; *Angew. Chem., Int. Ed. Engl.* **1988**, *27*, 759.

(10) (a) Mingos, D. M. P. *Acc. Chem. Res.* **1984**, *17*, 311. (b) Lauher, J. W. *J. Am. Chem. Soc.* **1979**, *100*, 5305. (c) Teo, B. K. *Inorg. Chem.* **1984**, *23*, 1251. (d) Teo, B. K.; Longoni, G.; Chung, F. R. K. *Ibid.* **1984**, *23*, 1257.

Table I. Structurally Characterized, Cubic Clusters of First-Row Transition Metals and Their Electron Counts

compd	skeletal electrons	metal electrons	ref
$\text{Ni}_8(\mu_4\text{-PPh})_6(\text{CO})_8$	120	68	6a
$\text{Ni}_8(\mu_4\text{-S})_6(\text{PPh}_3)_6\text{Cl}_2$	118	66	6b
$\text{Ni}_8(\mu_4\text{-PPh})_6(\text{PPh}_3)_4\text{Cl}_4$	116	64	6c
$\text{Ni}_8(\mu_4\text{-PPh})_6(\text{PPh}_3)_4$	112	68	6d
$\text{Co}_8(\mu_4\text{-S})_6(\text{SPh})_8^{4-5-}$	108, 109	52, 53	6e
$\text{Ni}_9(\mu_4\text{-Te})_6(\text{PET}_3)_8$	130	78	3
$\text{Ni}_9(\mu_4\text{-As})_6(\text{PPh}_3)_5\text{Cl}_3$	121	69	12

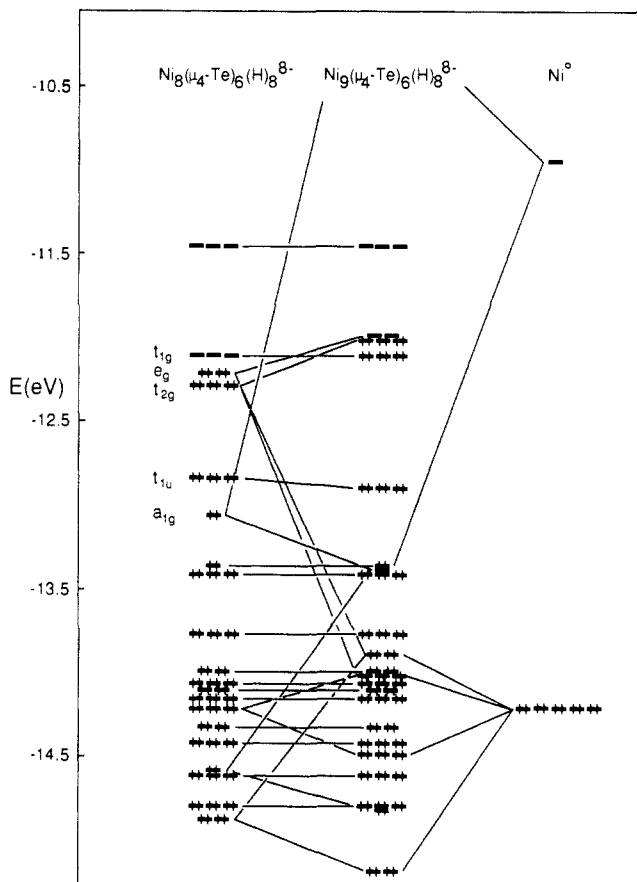
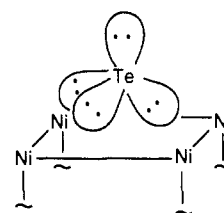


Figure 1. Interaction of the face-capped, cubic nickel cluster $\text{Ni}_8(\mu_4\text{-Te})_6(\text{H})_8^{8-}$ with Ni^0 to give $\text{Ni}_9(\mu_4\text{-Te})_6(\text{H})_8^{8-}$, a model for the experimentally observed, nickel-centered $\text{Ni}_9(\mu_4\text{-Te})_6(\text{PET}_3)_8$ cluster.

Assuming the Te electrons are directed toward the corners of a tetrahedron (as shown in 4) makes the face-capping tellurium a



4

six-electron donor. Taken together, the six telluriums contribute 36 electrons to the cluster. Since Ni is a d^{10} transition metal and the eight nickels must carry 12 positive charges to balance the charge on Te, the eight nickels provide $8 \times 10 - 12 = 68$ cluster electrons. If the central Ni donates all its electrons and each phosphine is regarded as a two-electron donor, the total cluster electron count is $36(\text{Te}_6^{12-}) + 68(\text{Ni}_8^{12+}) + 10(\text{Ni}^0) + 8 \times 2(8\text{PET}_3) = 130$. Apparently, the $\text{Ni}_9(\mu_4\text{-Te})_6(\text{PET}_3)_8$ cluster is electron-precise, and we might expect it to show optimum met-

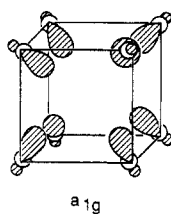
al-metal and metal-ligand bonding. Nonetheless, the variety of electron counts displayed in Table I implies that the cubic clusters have a number of electronic energy levels closely spaced near the HOMO-LUMO gap. As a consequence, cluster electron counts are sensitive to details of the metals and their ligand sets. We should not be surprised to find several possible electron counts for the known $\text{Ni}_9(\mu_4\text{-Te})_6(\text{PEt}_3)_8$ molecule and for our proposed $\text{Ni}_8\text{Te}(\mu_4\text{-Te})_6(\text{L})_8$ cluster.

Bonding to Interstitial Atoms

Figure 1 shows the orbital interactions important in bonding the central nickel atom, Ni^c , inside a $\text{Ni}_9(\mu_4\text{-Te})_6(\text{H})_8^{8-}$ model for the experimentally known cluster, $\text{Ni}_9(\mu_4\text{-Te})_6(\text{PEt}_3)_8$. On the left of the figure are the orbitals of the empty $\text{Ni}_8(\mu_4\text{-Te})_6(\text{H})_8^{8-}$ framework, on the right are the 4s and 3d orbitals of the central Ni atom, and in the center of Figure 1 are the orbitals of the composite cluster, $\text{Ni}_9(\mu_4\text{-Te})_6(\text{H})_8^{8-}$. The 3p orbitals of Ni^c are too high in energy to appear in the figure and make a minimal contribution to the chemical bonding in $\text{Ni}_9(\mu_4\text{-Te})_6(\text{H})_8^{8-}$.

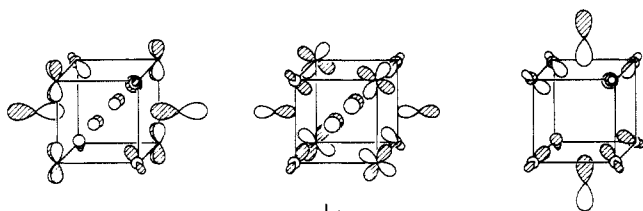
Since the orbitals of $\text{Ni}_8(\mu_4\text{-Te})_6(\text{H})_8^{8-}$ are very similar to those of $\text{Co}_8(\mu_4\text{-S})_6(\text{SR})_8$, discussed by Burdett and Miller for their analysis of pentlandite minerals,¹¹ only the orbitals near the HOMO-LUMO gap and those likely to interact strongly with the central atom are highlighted here. These orbitals are important in two ways: (1) they will interact directly with orbitals on the central atom, and (2) they may move above or below the HOMO for the empty cluster and substantially change bonding within the framework by becoming empty or filled. For a detailed derivation of orbitals for the empty, cubic cluster from the orbitals of two M_4 squares and an octahedron of six chalcogens, the reader is referred to ref 11.

Orbitals near the HOMO-LUMO gap of $\text{Ni}_8(\mu_4\text{-Te})_6(\text{H})_8^{8-}$ and likely to interact strongly with s, p, or d orbitals of the central atom are labeled on the left of Figure 1 according to their symmetries in the octahedral point group. Since atomic s, p, and d orbitals have a_{1g} , t_{1u} , and $t_{2g} + e_g$ symmetries in an octahedral environment, only cluster orbitals of these symmetries will interact with orbitals of the central atom. The highest energy, filled, $\text{Ni}_8(\mu_4\text{-Te})_6(\text{H})_8^{8-}$ orbital of a_{1g} symmetry, labeled to the left of Figure 1, is drawn out in 5. In a local coordinate system with



5

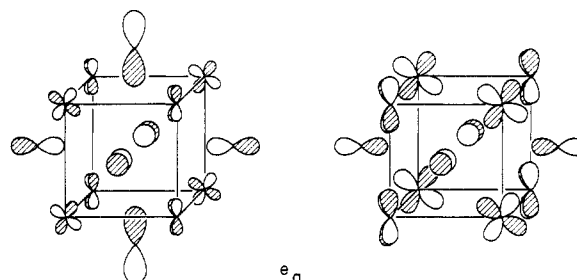
the z axes parallel to the Ni-H bonds, a_{1g} has mainly Ni z^2 character and is Ni-Ni bonding along the edges of the cube. Its antibonding character between each nickel and its terminal ligand is minimized by hybridization away from the ligand and toward the cube's center. The three degenerate t_{1u} levels are shown in 6 and are composed of Ni z^2 , with some xz and yz contributions



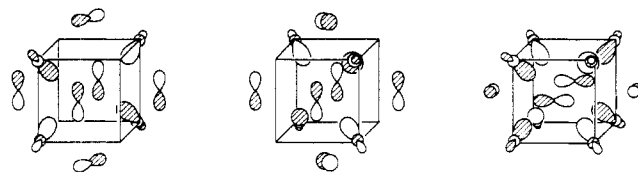
6

mixed in. Two members of the set have a nodal plane perpendicular to two faces of the cube and containing opposite corners. The third t_{1u} level has a horizontal nodal plane bisecting the front and back faces of the cube. Thus, the t_{1u} levels of the empty octahedral cluster are composed of metal z^2 , xz , and yz orbitals, arranged with the symmetry of a p orbital located at the cube center. A substantial contribution from 5p orbitals on the face-capping telluriums gives the t_{1u} levels shown in 6 a weak Ni-Te bonding character.

The same type of "united atom" view of the cluster used to describe the nodal structure of the t_{1u} levels can also be used to understand the relative phases of atomic orbitals that make up the e_g and t_{2g} levels, shown in 7 and 8. The e_g levels are composed



7



8

of Ni xz and yz components with contributions from tellurium p. The phases of the Te p orbitals are easily seen to correspond to the symmetry of z^2 and $x^2 - y^2$ orbitals located at the cube center. The coefficients of the Ni orbitals reflect the same symmetry, although metal contributions for one member of the pair are small as the nickels are located almost exactly in the nodal cone of a centrally located z^2 orbital. Similar to the e_g set, the cluster t_{2g} orbitals shown in 8 have two perpendicular nodal planes and a nodal structure analogous to metal xz , yz , and xy levels. The weakly bonding character of the PhP-NiL ($L = \text{Cl}, \text{CO}, \text{PPh}_3$) interaction carried by the e_g and t_{2g} levels is verified by experimental PhP-NiL bond lengths in the series of compounds $\text{Ni}_8(\mu_4\text{-PPh})_6(\text{CO})_8$, $\text{Ni}_8(\mu_4\text{-PPh})_6(\text{PPh}_3)_4\text{Cl}_4$, and $\text{Ni}_8(\mu_4\text{-PPh})_6(\text{PPh}_3)_4$. $\text{Ni}_8(\mu_4\text{-PPh})_6(\text{CO})_8$ has 120 framework electrons, the same electron count shown on the left of Figure 1, and P-Ni bond lengths of 2.17–2.19 Å.^{6a} As the e_g and t_{2g} levels are emptied for $\text{Ni}_8(\mu_4\text{-PPh})_6(\text{PPh}_3)_4\text{Cl}_4$ (116 electrons) and $\text{Ni}_8(\mu_4\text{-PPh})_6(\text{PPh}_3)_4$ (112 electrons), PhP-NiL bonds expand slightly to 2.20–2.22^{6c} and 2.24–2.28 Å.^{6d}

Our united atom trick for visualizing the cluster MO's also tells us directly which orbitals of the central metal will interact with which orbitals of the cluster. The spherically symmetric Ni^c 4s orbital will interact only with cluster a_{1g} levels. The a_{1g} orbital drawn in 5 has its lobes pointing toward the central Ni and a moderately good energy match with Ni 4s, so their interaction is strong. The resulting bonding orbital in fact contributes more than any other single level to Ni-Ni^c bonding. Although the cluster t_{1u} levels interact with Ni^c 3p orbitals to some extent, their energy differences are too large to produce significant interactions (all occupied cluster levels contain only 4.8% of the total Ni^c 4p). When the cluster t_{2g} levels interact with Ni^c xz , yz , and xy orbitals, they form lower energy bonding and higher energy antibonding combinations. Although the antibonding combination rises to high enough energy to become partially unoccupied, the net interaction is still destabilizing. Of the Ni^c d orbitals, the e_g pair contributes the most to Ni^c bonding as the cluster-Ni^c antibonding e_g set is

(11) Burdett, J. K.; Miller, G. J. *J. Am. Chem. Soc.* 1987, 109, 4081.

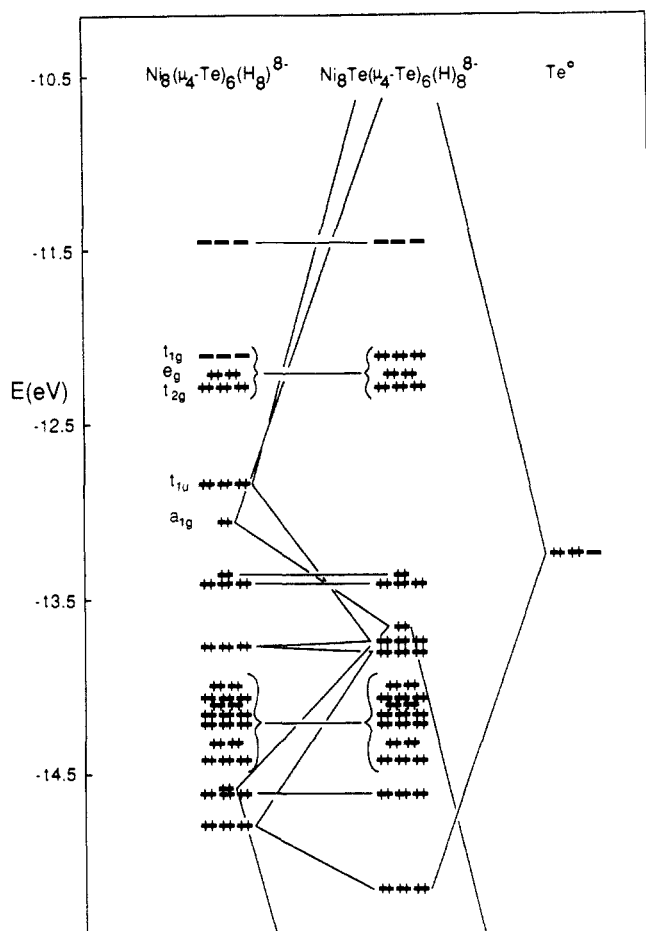
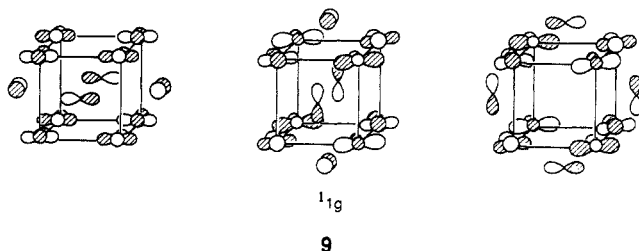


Figure 2. Interaction of the face-capped, cubic nickel cluster $\text{Ni}_8(\mu_4\text{-Te})_6(\text{H})_8^{8-}$ with Te^0 to give $\text{Ni}_8\text{Te}(\mu_4\text{-Te})_6(\text{H})_8^{8-}$, a hypothetical, Te-centered cluster related to the solid-state CsCl structure.

pushed to high enough energy to become empty. Thus, the bulk of the bonding of Ni^0 at the center of the cubic cluster is carried through the Ni^0 4s plus cluster a_{1g} orbital combinations, with an additional, small contribution from orbitals of e_g symmetry.

One other major change in cluster bonding occurs when the central nickel interacts with the $\text{Ni}_8(\mu_4\text{-Te})_6(\text{H})_8^{8-}$ cluster: the previously empty t_{1g} set becomes occupied. The t_{1g} orbitals are drawn out in 9 and have net Ni–Ni antibonding character. The



effect on metal–metal bonding of the t_{1g} and t_{2g} levels is seen by contrasting experimentally observed Ni–Ni distances in $\text{Ni}_9(\mu_4\text{-Te})_6(\text{PEt}_3)_8$ (130 cluster electrons) and $\text{Ni}_9(\mu_4\text{-As})_6(\text{PPh}_3)_5\text{Cl}_3$ (121 cluster electrons). Ni–Ni distances contract from 2.84–2.87 Å when t_{1g} and t_{2g} are occupied (for $\text{Ni}_9(\mu_4\text{-Te})_6(\text{PEt}_3)_8$),^{3a} to 2.77–2.85 Å when t_{1g} is singly occupied and t_{2g} is empty (for $\text{Ni}_9(\mu_4\text{-As})_6(\text{PPh}_3)_5\text{Cl}_3$).¹² The large energy gap below the t_{1g} levels, as well as their predominantly Ni–Ni antibonding character, suggests that 120 is an alternative electron count for the $\text{Ni}_9(\mu_4\text{-Te})_6(\text{L})_8$ cluster.

Table II. Decrease in Ni–Te Overlap Populations When the Empty Cluster $\text{Ni}_8(\mu_4\text{-Te})_6(\text{H})_8^{8-}$ Is Centered by Te ($\text{Ni}_8\text{Te}(\mu_4\text{-Te})_6(\text{H})_8^{8-}$, Te-Centered) or by Ni ($\text{Ni}_9(\mu_4\text{-Te})_6(\text{H})_8^{8-}$, Ni-Centered) (Contributions for All Orbitals of Selected Symmetries Also Presented)

	empty	Te-centered	Ni-centered
total	0.372	0.324	0.356
t_{1u}	0.135	0.099	0.130
a_{1g}	0.030	0.015	0.023
e_g	0.041	0.041	0.034
t_{2g}	0.072	0.072	0.070

Changing the terminal ligands from hydrides to chloride or carbonyl ligands changes preferred electron counts only slightly. Calculated orbital energies for the model compound $\text{Ni}_9(\mu_4\text{-Te})_6(\text{Cl})_8^{8-}$ show a moderately large 0.5-eV gap for an electron count of 126. This new energy gap is created as the chloride p orbitals stabilize the t_{1g} levels by mixing to reduce the Ni–Cl antibonding interaction. Thus, 126 and 120 are good electron counts for the face-capped, cubic cluster with terminal π -donor ligands. Terminal π -acceptor ligands modify the ordering of the t_{1g} , t_{2g} , and e_g levels without introducing additional, large energy gaps.

Figure 2 shows that the bonding between the cubic cluster framework and a central main-group atom such as Te is very different from framework bonding to a central transition-metal atom. The left side of Figure 2 illustrates the levels of $\text{Ni}_8(\mu_4\text{-Te})_6(\text{H})_8^{8-}$, the right side shows the Te 5p orbitals, and the middle represents the energy levels of the hypothetical $\text{Ni}_8\text{Te}(\mu_4\text{-Te})_6(\text{H})_8^{8-}$ cluster with 130 skeletal electrons. The tellurium 5s orbital is too low in energy to fit on the figure, but its effect is represented by energy changes among the framework a_{1g} levels upon interaction of $\text{Ni}_8(\mu_4\text{-Te})_6(\text{H})_8^{8-}$ and Te. Since the Te 5s level is at much lower energy than the Ni 4s (–20.8 eV versus –10.95 eV for Ni in the extended Hückel calculations), the Te 5s interacts more strongly and with more framework a_{1g} orbitals than the Ni 4s does. Consequently, the antibonding a_{1g} partner at high energy is concentrated mainly on the cubic framework of $\text{Ni}_8\text{Te}(\mu_4\text{-Te})_6(\text{H})_8^{8-}$. The Te 5p orbitals also fall in the same energy range as a dense block of framework orbitals with matching t_{1u} symmetry. The energy match between Te 5p and framework t_{1u} levels, as well as the strong overlap between Te^0 and the Te 5p component of framework t_{1u} , guarantees a strong bonding interaction. The result is a substantially lowered energy of the Te-centered cluster, with the framework t_{1u} levels pushed above the cluster HOMO and the t_{1g} levels fully occupied.

Although the orbital interactions described above point to significant stability for the Te-centered cluster, overlap populations (indicators of bond order) show a decrease in framework bonding upon centering the empty cluster with Ni or with Te. Total Ni–Ni overlap populations are very small and indicate extremely weak or absent Ni–Ni bonding for the empty (Ni–Ni overlap population of 0.036), the Ni-centered (0.010), and the Te-centered clusters (0.003). Ni–Ni bonding in both the Ni- and Te-centered clusters differs from that in the empty cluster primarily by virtue of the occupied, Ni–Ni antibonding t_{1g} levels. In the Te-centered cluster, the t_{1g} orbitals alone are responsible for half the drop in Ni–Ni overlap populations upon adding the central atom. The a_{1g} orbital (5) that is emptied upon interaction with Te 5s accounts for most of the remaining drop in Ni–Ni overlap population.

Table II shows Ni–Te overlap populations for the empty, the Te-centered, and the Ni-centered clusters. Total Ni–Te overlap populations, as well as contributions from all orbitals of the indicated symmetries are reported. Like Ni–Ni bonding, Ni–Te bonding is reduced for both the Ni- and Te-centered molecules compared to the empty cluster. For $\text{Ni}_9(\mu_4\text{-Te})_6(\text{H})_8^{8-}$, the a_{1g} and e_g levels contribute most to the decrease in Ni–Te overlap population. For the $\text{Ni}_8\text{Te}(\mu_4\text{-Te})_6(\text{H})_8^{8-}$ cluster, the 13% decrease in Ni–Te bonding is due to levels of both a_{1g} and t_{1u} symmetries. Hence, Ni–Te bonding is disrupted in both the Ni- and Te-centered clusters by direct orbital interactions, and the small degree of Ni–Ni bonding in the empty $\text{Ni}_8(\mu_4\text{-Te})_6(\text{H})_8^{8-}$ cluster

(12) Fenske, D.; Merzweiler, K.; Ohmer, J. *Angew. Chem.* **1988**, *100*, 1572; *Angew. Chem., Int. Ed. Engl.* **1988**, *27*, 1512.

Table III. Parameters¹⁴ for H, Te, and Ni Used in the Extended Hückel¹³ Calculations

atom	orbital	H_{ii} (eV)	ζ_1^a (C ₁)	ζ_2^a (C ₂)
H	1s	-13.6	1.3	
Te	5s	-20.8	2.51	
	5p	-13.2	2.16	
Ni	4s	-10.95	2.1	
	4p	-6.27	2.1	
	3d	-14.2	5.75 (0.5798)	2.30 (0.5782)

^a Coefficients used in a double- ζ expansion of the 3d orbitals.

framework is destroyed by centering the cluster with either Ni or Te as electrons are redistributed into the t_{1g} levels.

Unlike the $Ni_9(\mu_4\text{-Te})_6(\text{H})_8^{8-}$ cluster, $Ni_8\text{Te}(\mu_4\text{-Te})_6(\text{H})_8^{8-}$ compensates for the lost framework bonding by incorporating the central Te as an integral part of the cluster. Whereas the Ni^c -Ni overlap population (0.070) in $Ni_9(\mu_4\text{-Te})_6(\text{H})_8^{8-}$ indicates only weak bonding between Ni^c and framework nickels and the Ni^c -Te overlap population (-0.001) indicates no Ni^c -Te bonding, Te^c bonds strongly to both Ni and Te in $Ni_8\text{Te}(\mu_4\text{-Te})_6(\text{H})_8^{8-}$. The Te^c-Ni overlap population of 0.206 is comparable to the overlap population describing (face-capping) Te-Ni bonds (0.324). Furthermore, the Te^c-Te overlap population of 0.163 unambiguously indicates a substantial bonding interaction between Te^c and each of the face-capping telluriums. Thus, the loss of framework bonding upon centering the empty framework by Te^c is compensated by strong Te^c-Ni and Te^c-Te bonding.

Since the orbitals grouped near the HOMO-LUMO gap are weakly Ni-Ni antibonding and Ni-Te bonding, the picture of framework bonding described above is altered little by emptying the eight highest occupied levels in Figure 2. The large energy gap below t_{2g} implies that 114, as well as 130, is an optimum electron count for $Ni_8\text{Te}(\mu_4\text{-Te})_6(\text{L})_8$. The figure also implies that electron counts of 124 and 120 give closed-shell clusters; however, the precise ordering of t_{1g} , e_g , and t_{2g} probably varies depending upon the nature of the terminal ligands. Exploratory calculations with terminal chloride or carbonyl ligands indicate a 0.71-eV HOMO-LUMO gap at 120 electrons for $L = \text{Cl}^-$, with no substantial differences from Figure 2 observed for $L = \text{CO}$.

Conclusions

The central nickel atom, Ni^c , in the experimentally known cluster, $Ni_9(\mu_4\text{-Te})_6(\text{PEt}_3)_8$, acts as a true interstitial by providing electrons without bonding strongly to the $Ni_8(\mu_4\text{-Te})_6$ cluster framework. Weak Ni^c -Ni bonding is carried primarily through the orbitals of a_{1g} and, to a lesser extent, e_g symmetries. Emptying

the highest occupied t_{1g} and t_{2g} levels of their 10 electrons should strengthen framework Ni-Ni and Ni-Te bonding and suggests that 120 is also a good electron count for the metal-centered cluster.

In contrast, Te^c is incorporated as an integral part of the $Ni_8\text{Te}(\mu_4\text{-Te})_6(\text{H})_8^{8-}$ model cluster by bonding strongly to both the Ni and Te atoms of the framework. Calculated energies, orbital interactions, and overlap populations, measures of bond orders, all indicate the stability of the Te-centered cluster $Ni_8\text{Te}(\mu_4\text{-Te})_6(\text{L})_8$. Energy gaps near the HOMO of Figure 2 indicate that 130 and 114 are optimum electron counts for this cluster of octahedral symmetry. The close grouping of orbitals near the HOMO of Figure 2, as well as the variety of cluster electrons counts for the empty, cubic clusters summarized in Table 1, imply the possibility of other electron counts depending on details of the ligand set.

Acknowledgment. I am grateful to the University of Oklahoma Department of Chemistry and Biochemistry for supporting this research, to University Computing Services for making computer resources available through the College of Arts and Sciences, and to Margaret Smith of the Instructional Services Center for providing the illustrations.

Appendix

All calculations were performed by use of the extended Hückel method with weighted H_{ij} 's¹³ and parameters (see Table III) taken from previous calculations.¹⁴ Ni-Ni (2.85 Å) and Ni-Te (2.55 Å) bond lengths are average distances reported in ref 4, and the Ni-H distance of 1.6 Å is the approximate M-H distance for first-row transition-metal hydrides.¹⁵ For both the Ni-centered and Te-centered clusters, calculations were performed on idealized structures with perfectly cubic arrays of Ni and octahedral arrangements of the face-capping telluriums. Hydride ligands were oriented along 3-fold axes to preserve the overall octahedral symmetry.

(13) (a) Wolfsberg, M.; Helmholz, L. *J. Chem. Phys.* **1952**, *20*, 837. (b) Hoffmann, R.; Lipscomb, W. N. *J. Chem. Phys.* **1962**, *36*, 2179. (c) Jordan, T.; Smith, H. W.; Lohr, L. L., Jr.; Lipscomb, W. N. *J. Am. Chem. Soc.* **1963**, *85*, 846. (d) Ammeter, J. H.; Bürgi, H.-B.; Thibeault, J. C.; Hoffmann, R. *J. Am. Chem. Soc.* **1978**, *100*, 3686.

(14) (a) Summerville, R. H.; Hoffmann, R. *J. Am. Chem. Soc.* **1976**, *98*, 7240. (b) Canadell, E.; Mathey, Y.; Whangbo, M.-H. *J. Am. Chem. Soc.* **1988**, *110*, 104.

(15) (a) Teller, R. G.; Bau, R. *Struct. Bonding (Berlin)* **1981**, *44*, 12. (b) McNeill, E. A.; Scholer, F. R. *J. Am. Chem. Soc.* **1977**, *99*, 6243. (c) LaPlaca, S. J.; Hamilton, W. C.; Ibers, J. A.; Davison, A. *Inorg. Chem.* **1969**, *8*, 1928.